

## Space weather activities at SERC for IHY: MAGDAS

Kiyohumi Yumoto\* and the MAGDAS group

*Space Environment Research Center, Kyushu University, Hakozaki 6-10-1, Higashi-ku,  
Fukuoka 812-8581, Japan*

**Abstract.** We will introduce MAGDAS project of Space Environment Research Center (SERC), Kyushu University (KU) for space weather. The new MAGDAS data can be used to monitor global electromagnetic and plasma environment change in geospace, and then to bring about a better understanding of the complex and compound Sun-Earth system. The SERC also conducts daily space weather “now casting”, to train and educate KU students, and to globally disseminate space weather information to the scientific community and the general public.

**Keywords :** MAGDAS – space weather – global ionospheric current – plasma mass density – ionospheric electric field – local education – global outreach – data service

### 1. Introduction

The International Heliophysical Year (IHY) is an extensive international programme to study the universal physical processes in the heliospace for a better understanding of the Sun-heliosphere system during 2007-09. The IHY will continue the legacy of the International Geophysical Year (IGY) during 1957-58 by extending the physical realm from geospace to heliospace, recognizing the enormous progress made over the past 50 years. There are four key elements of IHY: 1) Science; coordinated investigation programmes or CIP's conducted as campaigns to investigate specific scientific questions. 2) Instrument development; the IHY/UNBSS programme. 3) Public outreach to communicate the beauty, relevance and significance of space science to the general public and students. 4) The IGY Gold Club programme to identify and honour the scientists who worked for the IGY programme (see <http://www.unoosa.org/oosa/en/SAP/bss/ihy2007/index.html>).

---

\*yumoto@serc.kyushu-u.ac.jp

The IHY organization in Japan was recognized to conduct the STPP (Solar Terrestrial Physics Programme) Sub-Committee under the International Subgroup of the Earth and Planetary Science Committee, Science Council of Japan, in 2006 (see <http://www2.nict.go.jp/y/y223/sept/IHY/IHY-e.html>). Four global ground-based observation projects (MAGDAS; Kyushu Univ., Muon Detector; Shinshu Univ., IPS; Nagoya Univ., CHAIN; Kyoto Univ.) contribute to IHY Science and instrument development. Public outreach is carried out by NICT Space Weather Center, Tokyo through the Network of (ISES; International Space Environment Services). The IGY Gold Club members are also nominated from Japan. In June 2007, National Astronomical Observatory in Japan will host an UN/ESA/NASA Workshop on Basic Space Science and IHY 2007 in Tokyo.

The Space Environment Research Center (SERC), Kyushu university is constructing Network Stations for global observations and Modeling Stations for integrated simulation/empirical modeling to bring about a better understanding of the multi-scale couplings in the complex and composite Sun-Earth system during the IHY period. By using the new MAGDAS data, we can conduct a real-time monitoring and modeling of (1) the global 3-dimensional current system to know electromagnetic couplings of the region 1 and 2 field-aligned currents, auroral electrojet current, Sq current, and equatorial electrojet current, and (2) the ambient plasma density for understanding the global electromagnetic and plasma environment responses in geospace to the solar wind changes. From the FM-CW radar observation along the 210° magnetic meridian, we can deduce (3) electric fields in the eastwest direction from the ionospheric plasma Doppler velocity to clarify how polar electric fields penetrate into the equatorial ionosphere.

In the present paper, we will introduce briefly our real-time data acquisition and analysis system of MAGDAS/CPMN, preliminary results obtained from this system, local education, global outreach and data service at SERC ([http://www.serc.kyushu-u.ac.jp/index\\_e.html](http://www.serc.kyushu-u.ac.jp/index_e.html)).

## 2. MAGDAS/CPMN system

The Circum-pan Pacific Magnetometer Network (CPMN) was constructed by Kyushu University in collaboration with about 30 international organizations along the 210° magnetic meridian (MM) and the magnetic equator during the international Solar Terrestrial Energy Programme (STEP) period (1990-97) (see Yumoto and 210° MM group, 1995 and 1996, Yumoto and CPMN group, 2001). For space weather study and application, the SERC, Kyushu University is now deploying a new real-time MAGDAS (MAGnetic Data Acquisition System) in the CPMN region, and the FM-CW radar array along the 210° MM. Fifty new fluxgate-type magnetometers and their data acquisition system from overseas sites to Japan are being deployed by the SERC, Kyushu University starting from 2005.

MAGDAS/CPMN is roughly divided into two portions. MAGDAS-A system is a new

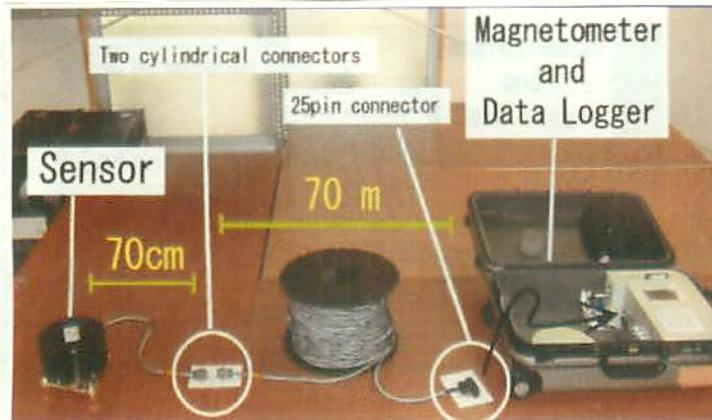
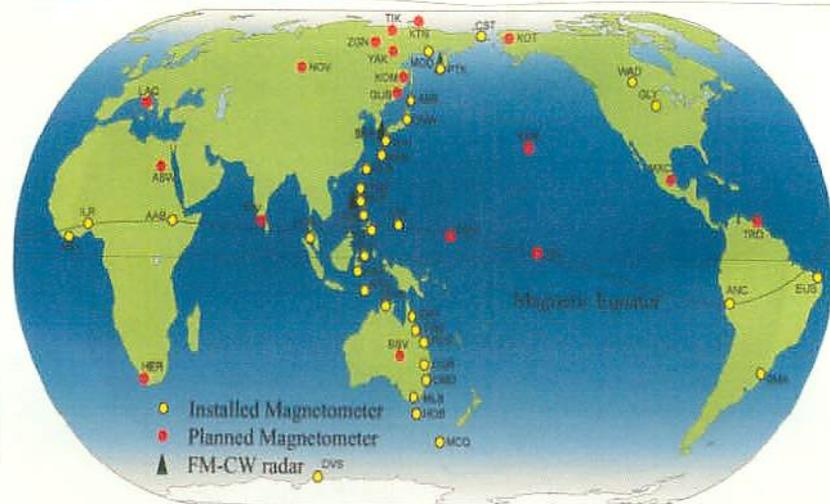


Figure 1. MAGDAS magnetometer system.

magnetometer system installed at the CPMN stations, while MAGDAS-B is data acquisition and monitoring system installed at SERC. The new MAGDAS-A system consists of 3-axial ring-core sensors, tilt-meters and thermometer in sensor unit, fluxgate-type magnetometer, data logger/transfer units, and power unit as shown in Fig. 1. Magnetic field digital data ( $H+\delta H$ ,  $D+\delta D$ ,  $Z+\delta Z$ ,  $F+\delta F$ ) are obtained with the sampling rate of 1/16 seconds, and then the 1-sec averaged data are transferred from the overseas stations to the SERC, Japan in real time (see Yumoto and MAGDAS group, 2006). The ambient magnetic fields, expressed by horizontal (H)-, declination (D)-, and vertical (Z)-components, are digitized by using the field-canceling coils for the dynamic range of  $\pm 64,000\text{nT}/16\text{bit}$ . The magnetic variations ( $\delta H$ ,  $\delta D$ ,  $\delta Z$ ) subtracted from the ambient field components (H, D, Z) are further digitized by a 16-bit A/D converter. Two observation ranges of  $\pm 2,000\text{nT}$  and  $\pm 1,000\text{nT}$  can be selected for high-and low-latitude stations, respectively. The total field ( $F+\delta F$ ) is estimated from the  $H+\delta H$ ,  $D+\delta D$ , and  $Z+\delta Z$  components. The resolutions of MAGDAS data are  $0.061\text{nT}/\text{LSB}$  and  $0.031\text{nT}/\text{LSB}$  for  $\pm 2,000\text{nT}$  and  $\pm 1,000\text{nT}$  range, respectively. The estimated noise level of the MAGDAS magnetometers is less than  $0.1\text{nTp-p}$ . The long-term inclinations (I) of the sensor axes can be measured by two tilt-meters with resolution of 0.2 arcsec. The temperature (T) inside the sensor unit is also measured. The GPS signals are received to adjust the standard time inside the data logger/transfer unit. These data are logging in the Compact Flash Memory Card of 1 GB. The data transferring unit transfers the 1-sec averaged data ( $H+\delta H$ ,  $D+\delta D$ ,  $Z+\delta Z$ ,  $F+\delta F$ ) in real time from the overseas stations to the SERC, Japan, by using three possible ways: Internet, Telephone line or Satellite phone line. The total weight of the MAGDAS magnetometer system is less than 15 kg. Every day, the data logger at an overseas site generates a file containing averaged 1-sec magnetic data (H, D, Z, F) and a file containing the averaged 1-min magnetic data and inclination and temperature data (I, T) of the magnetometer sensor. The file size of the 1-sec data is less than 1MB. The file size of the 1-min data is less than 50KB. The MAGDAS data are transferred from the overseas stations to the SERC, Japan, by using three possible ways a) Special line for INTERNET, b) Telephone line, and c) Satellite telephone line (see Yumoto, and MAGDAS group, 2006).



**Figure 2.** Map of 50 MAGDAS stations in the Circum-pan Pacific Magnetometer Network (CPMN) region.

MAGDAS magnetometers were installed at 19 stations along the  $210^\circ$  magnetic meridian in 2005 as shown in Fig. 2. In 2006, 7 and 8 MAGDAS magnetometers were installed along the magnetic equator and at middle latitudes, respectively.

### 3. Scientific objectives and preliminary results

MAGDAS system can obtain amplitude-time records of 4-component ordinary and induction-type magnetic field variations. The ordinary data (i.e. MAGDAS data (1)) can be used for studies of long-term variations, e.g. magnetic storm, auroral substorms, Sq, etc., while the induction-type data (i.e. MAGDAS data (2)) will be useful for studies of ULF waves, transient and impulsive phenomena. By using these new MAGDAS data, we can conduct a real-time monitoring and modeling of (1) the global 3-dimensional current system and (2) the ambient plasma density for understanding the global electromagnetic and plasma environment changes in geospace. From the FM-CW radar observation at  $L=1.26$ , we can also deduce (3) electric fields in the eastwest direction from the ionospheric plasma Doppler velocity.

#### 3.1 Ionospheric current patterns

In order to understand electromagnetic couplings of solar wind-magnetosphere-ionosphere-atmosphere system and its environment change, i.e. a coupling of the regions 1 and 2 field-aligned currents, auroral electrojet current, Sq current, and equatorial electrojet current, we will monitor the equivalent ionospheric current patterns obtained from the MAGDAS ordinary data as shown in Fig. 3. At high latitudes the ionospheric currents are joined with field-aligned currents (FAC) from the solar wind region into the

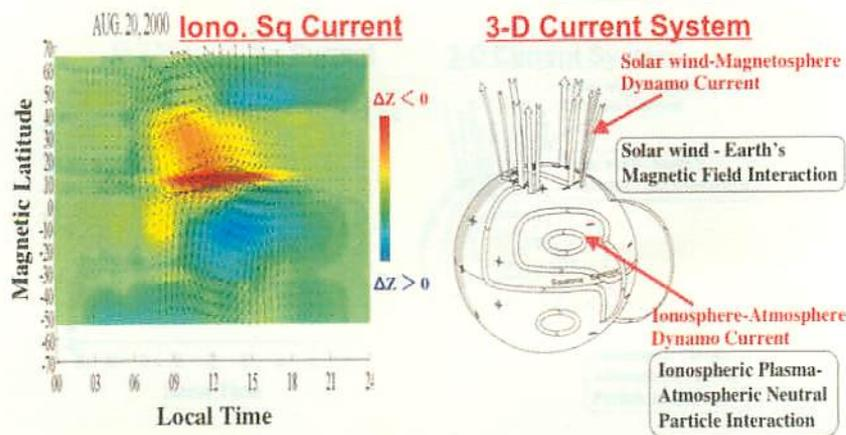


**Figure 3.** (Left) Global equivalent ionospheric current pattern obtained by ordinary MAGDAS/CPMN data. (Right) Three-dimensional current system in geospace.

magnetosphere, and the electrodynamics is dominated by the influences of solar wind-magnetosphere interaction processes. The total current flows is on the order of  $10^7$  A. On the other hand, the ionospheric current at middle and low latitudes is generated by the ionospheric wind dynamo, which produces global current vortices on the day-side ionosphere, i.e., counterclockwise in the northern hemisphere and clockwise in the southern hemisphere. The total current flow in each vortex is order of  $10^5$  A. There are strong electric fields at high latitudes, on the order of several tens of millivolts per meter or more depending on the magnetic activity. At middle and low latitudes electric fields are considerably smaller, typically a few millivolts per meter during magnetically quiet periods.

The left panel of Fig. 3 shows equivalent ionospheric current patterns obtained from the MAGDAS data (1) (Kohta et al. 2005). The vertical axis indicates magnetic latitudes of the MAGDAS stations, and the horizontal axis is the local time of the  $210^\circ$  magnetic meridian stations. The arrows indicate the 30-min averaged equivalent ionospheric current vectors obtained from  $90^\circ$  rotation of ground magnetic horizontal (H, D) variation vector, and the colour code indicates the negative and positive magnetic Z component. The 30-min averaged magnetic (H, D, Z) variations are calculated by subtracting each non-disturbed nighttime level. The equatorial electrojet can be seen at the dayside dip equator. There are twin vortices of Sq current, i.e., counter-clockwise and clockwise in the northern and southern hemisphere, respectively. The centres of Sq current patterns are sometimes not consistent with the maximum and minimum points of the Z component. During magnetic active periods the part of strong electric fields at high latitude can penetrate into middle and low latitudes, and then the global ionospheric current pattern must be reorganized strongly. In reality the current and electric fields at all latitudes are coupled, although those at high, middle and low latitudes have been often considered separately. By using the MAGDAS ionospheric current pattern, the global electromagnetic coupling processes at all latitudes will be clarified in near future.

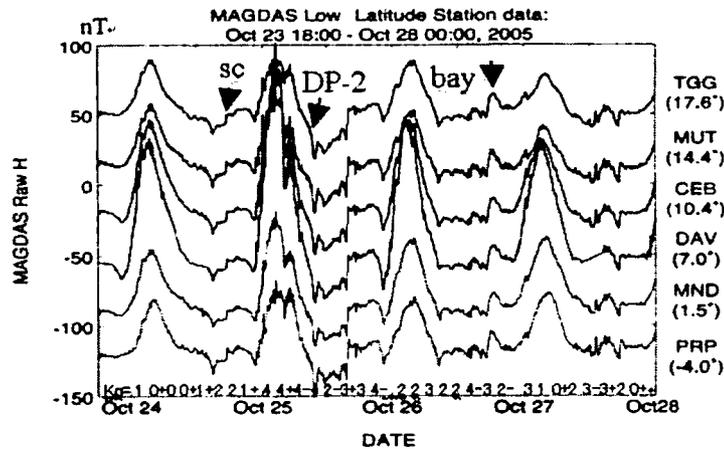


**Figure 4.** H-component amplitude-time records observed at the MAGDAS stations (TGG, MUT, CEB, and DAV in Philippines, MND, and PRP in Indonesia).

Fig. 4 shows one example of amplitude-time records of H-component magnetic fields observed at the MAGDAS stations (TGG, MUT, CEB, and DAV in Philippines, and MND and PRP in Indonesia) along the  $210^\circ$  magnetic meridian near the dip equator during five days of October 24–28, 2005 (see MAGDAS Home Page; <http://magdas.serc.kyushu-u.ac.jp/station/index.html>). Kp index is indicated at lower corner of the figure. We can see clear equatorial enhancements of about  $\geq 100$  nT near the magnetic equator at DAV (Dip Lat. =  $-0.65$ ), and global nature of sc, DP-2, and substorm bay variations. It is noteworthy that the magnetic variations along the  $210^\circ$  magnetic meridian show very similar amplitude-time forms.

On the other hand, Fig. 5 shows H-component amplitude-time records observed near the dip magnetic equator at DAV (Dip LAT =  $0.65$ ) and LKW ( $-1.88$ ) in Asian sector, at AAB ( $0.56$ ), ILR ( $-2.95$ ), and ABJ ( $-6.32$ ) in African sector, and EUS ( $-7.0$ ) in Southern American sector during October 1–5, 2006. Kp index is shown at lower corner of the figure. Not-similar equatorial enhancements can be seen at the different longitude stations. Further studies on the different variations near the magnetic equator are needed with respect to electrical conductivity at different longitudes and electric field penetration from polar ionosphere into the dip equator during magnetic active days.

It is vital to monitor equatorial electromagnetic phenomena for not only clarifying their occurrence mechanisms but also for studying magnetic storm as space weather. Aside from MAGDAS/CPMN, there is no monitoring system of the equatorial electrojet (meaning, there is no system that has stations located along the dip equator in sufficient numbers). It is important to construct a real-time monitoring system of temporal and long-term variations of equatorial magnetic disturbances associated with the equatorial electrojet and counter electrojet. Using MAGDAS/CPMN real-time data, Uozumi et al.

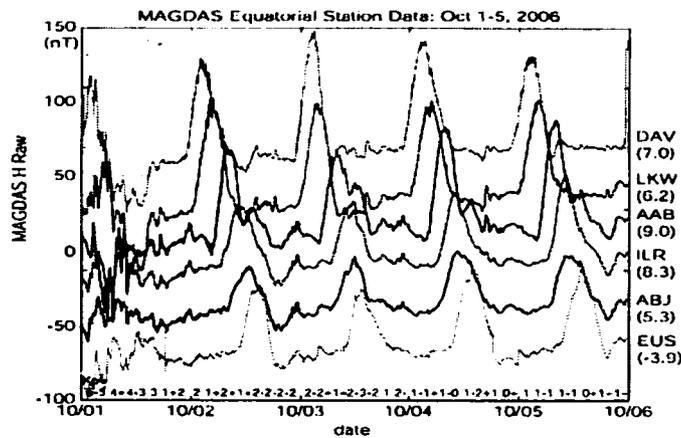


**Figure 5.** H-component amplitude-time records observed near the dip magnetic equator at DAV and LKW in Asian sector, at AAB, ILR, and ABJ in African sector, and at EUS in southern America sector.

(2007) proposed a basic algorithm to achieve the goals stated above, and also a new index: The EE-Index (EDst, EU and EL), to quantify the scale of disturbances.

### 3.2 Plasma mass density

The field line resonance (FLR) oscillations in the Earth's magnetosphere are excited by external source waves, and are so-called as ultra low frequency (ULF) waves (cf. Yumoto 1988). The amplitude of H-component magnetic variations observed at the ground stations reaches a maximum at the resonant point, and that its phase jumps by 180 degrees across the resonant point (see Yumoto 1985). The eigen-period of FLR oscillations is dependent upon the ambient plasma density and the magnetic field intensity in the region of geospace threaded by the field line, and the length of the line of force as shown in Fig. 6. When we observe the eigen-period of FLR and assume models for the latitude profiles of the magnetic field and the plasma density (with the equatorial density as a free parameter), we can estimate the plasma mass density in the inner magnetosphere. Therefore, the FLR oscillations are useful for monitoring temporal and spatial variations in the magnetospheric plasma density.

By using the ground-based network observations, we can identify the FLR phenomena and measure the fundamental field-line eigen-frequency by applying the dual-station H-power ratio method (Baransky et al. 1985) and the cross-phase method (Baransky et al. 1990, Waters et al. 1991) as shown in the left panel of Fig. 6, which have been established to identify the FLR properties. Applying these methods, Takasaki et al. (2006) discussed temporary variations of the plasma mass density during magnetic storms. From the ground-based observations at  $L \sim 1.4$  they found a significant decrease in the FLR frequency during a large magnetic storm as shown in Fig. 7. During 28–31 October, 2003,

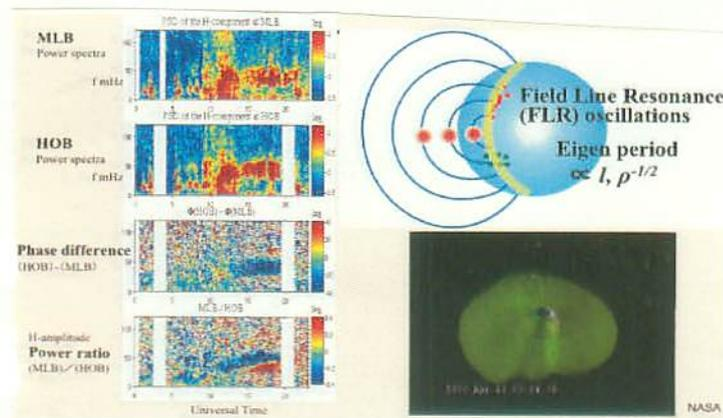


**Figure 6.** (Left) The FLR method to identify the eigen-frequency in phase difference and power ratio between power  $f$ - $t$  diagrams at two separated stations (Melbourne and Hobart). (Right) Schematic illustrations of FRL and plasmasphere by NASA.

a series of coronal mass ejections hit the magnetosphere and triggered two consecutive large storms. Three ground magnetometers at  $L = 1.32\sim 1.41$  recorded field-line resonances (FLRs) during this interval. The FLR frequencies decreased from 0600 LT on 31 October 2003 during the main phase of the second storm until 12 LT when the recovery phase of this storm began. After the decrease, the FLR frequencies increased to its value before the storm started at 0600 LT on 31 October in a few hours. The measured decrease in FLR frequency might indicate a relative increase in mass density along the field lines during the magnetic storm. On the other hand, the plasma number density in the ionosphere estimated from TEC values was similar in magnitude taken during quiet time. A possible explanation for the increase in mass density would be an uplift (outflow) of the heavy ions (e.g.,  $O^+$ ) from the ionosphere to the plasmasphere (see Tsurutani et al. 2006).

### 3.3 Ionospheric electric field

In order to investigate penetration mechanisms of the ionospheric electric fields from the polar into the equatorial ionosphere, we have built a FM-CW radar (HF radar of 2~42 MHz) system at Sasaguri, Fukuoka (G. M. Lat  $\theta = 23.2^\circ$ , G. M. Lon  $\lambda = 199.6^\circ$ ). The height of dipole antenna is 26 m. HF radio wave of 2~30 MHz is emitted in the vertical direction with 20 w power for ionosonde mode, while radio waves of central frequencies ( $f_0$ ; 2.5 and 8 MHz) for Doppler mode are emitted during night (09~21 UT=18~06 LT) and day time, respectively. The speed of sweep frequency and the sampling frequency are 100~1000 kHz/sec and 2000~20,000 Hz/sec, respectively. This system can measure the Doppler frequency ( $\Delta f$ ) of reflected radio wave from the ionized layer and the height of reflection layer with 10-sec sampling rate. From the observed vertical plasma drift

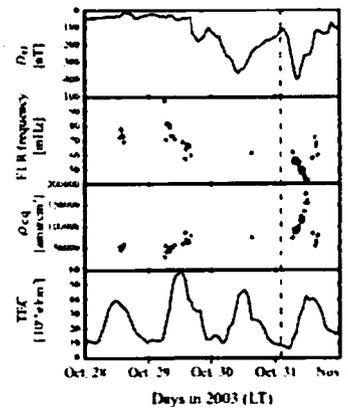


Figure 7. (From top to bottom) Dst index, FLR frequencies derived from ground observations at  $L \sim 1.4$ ,  $\rho_{eq}$  estimated from data in the second panel, and the total electron content (TEC). The dashed vertical line marks the beginning of the second magnetic storm (Takasaki et al. 2006).

velocity ( $v = -c\Delta f/2f_0$ ), we can deduce east-west component of electric field ( $E$ ) in the ionosphere, i.e.  $E = -v \times B_0$ , where  $B_0$  is the ambient magnetic field at Sasaguri.

The ionospheric electric field and its intensity at the time of SC are estimated as shown in Fig. 8. From top to bottom, the number density measured by the ACE satellite in the solar wind region, the H-component magnetic field variations at the CPMN station at Cebu near the magnetic equator, and the Doppler frequency of FM-CW radar at Sasaguri are shown as a function of amplitude-time records during 90 minute on November 4, 2003.

We selected 40 SC events that were identified by using a magnetometer at KUJ (G.M. Lat =  $23.6^\circ$ , G.M.Lon =  $203.2^\circ$ ) and the FM-CW radar during the period from 2002 to 2005. At first, we analyzed step-function like changes of the ionospheric electric fields during SC, and found that the ionospheric electric fields show eastward in daytime (06-20 LT) and westward in the nighttime (17-07 LT) as shown in Fig. 9. The averaged amplitude ranges of the electric fields are  $0.5\text{mV/m}$  in daytime and  $1.0\text{mV/m}$  in the nighttime. We compared step-function like changes of the electric fields with those of the magnetic fields at the time of SC, and found a positive correlation (correlation coefficient =  $0.70$ ) between the electric and magnetic field changes. We also compared the ionospheric electric fields with changes in the dynamic pressure ( $P_{sw}$ ) of the solar wind at the time of interplanetary shock event. There was a weak correlation (correlation coefficient =  $0.65$ ) between them, while no correlation was found between the electric fields of the solar wind ( $E_{sw}$ ) and the ionospheric electric fields. The ionospheric electric fields seem to depend mainly on the  $P_{sw}$ .

These observations suggest that the ionospheric electric fields at low latitudes during SC consist of dawn-to-dusk electric fields with the averaged  $0.75\text{mV/m}$  amplitude, which

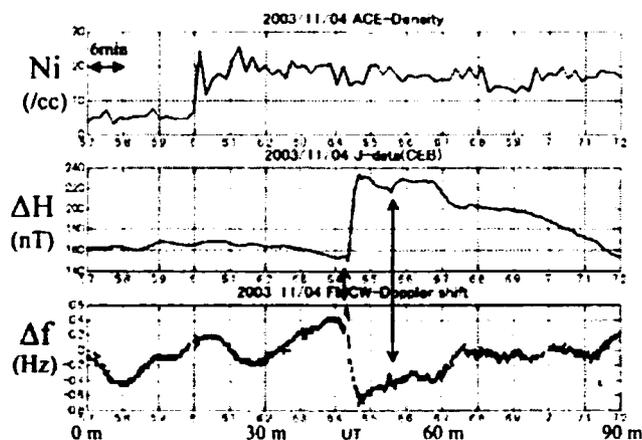


**Figure 8.** From top to bottom, the number density in the solar wind region, the H-component magnetic field at Cebu near magnetic equator, and the Doppler frequency of FM-CW radar at Sasaguri on November 4, 2003.

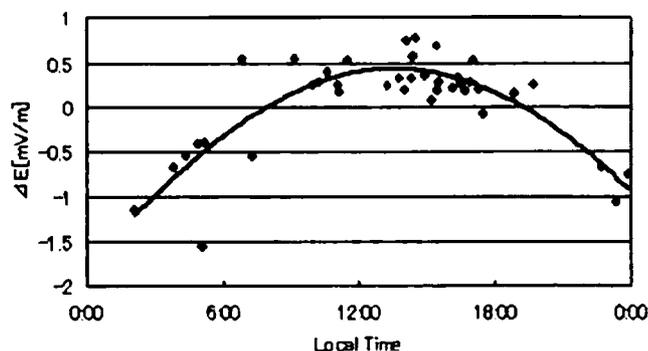


**Figure 9.** Local-time dependence of ionospheric electric fields of sc's at Sasaguri (Ikeda et al. 2006).

penetrate from the polar ionosphere into the equatorial ionosphere, and westward electric fields caused by global inward (compressional) ionospheric movements with the averaged amplitude of 0.25mV/m, which propagate across the magnetosphere.

#### 4. Local education, global outreach and database service

The SERC, Kyushu University (KU) conducts everyday space weather “now casting”. There are two main goals in this effort; (1) To train and educate KU students about the complexities of the Sun-Earth system so that they can become space weather forecasters in the future. (2) To globally disseminate space weather information from SERC as a service to the scientific community and the general public.

In order to understand the complexities of the Sun-Earth system, KU students analyze data in the four regions; (1) solar surface, (2) solar wind, (3) geospace, and (4) the Earth's surface. Using real-time public data from SOHO Real Time Movies, Solar Monitor, NASA/GSFC/SDAC, SEC's Anonymous FTP Server, they check daily sun spot number, locations of active regions and coronal holes, and identify events of flare: GOES X-Ray Flux, CME: SOHO/LASCO-C2, 3, and proton event: GOES Proton Flux. Analyzing ACE Real Time Data, KU students read solar wind (speed, density, temperature) and interplanetary magnetic field (IMF: Bt, Bz, Phi), and identify events of sector boundary, CIR, CME, and shock/discontinuity. For understanding magnetic activities in geospace and on the Earth's surface, storms and substorms are also analyzed by using Dst index (Kyoto Univ.), Kp index (NOAA), EE Index (Equatorial Electrojet: SERC) and Magnetic Pulsation Index (Pc 3, 4, and 5: SERC). Every morning KU students create a Space Weather report and then discuss it with the staff at SERC for local training and education. The report and its details are disseminated on the SERC Home page (<http://www.serc.kyushu-u.ac.jp>) for global outreach of space weather information from SERC.

MAGDAS magnetometers were installed at 19 and 15 stations along the 210° MM in 2005 and the magnetic dip equator in 2006, respectively, including East Asia, Pacific Ocean and Micronesian Islands, and South America and Africa. After corrections obtained from the MAGDAS data at SERC, MAGDAS collaborators have access to a SERC server, in which the corrected data are stored, and get 1-min and 1-sec digital data. MAGDAS data is available to researchers via the Internet, after direct inquiry with SERC. SERC will offer to the scientific community the MAGDAS database for collaborative works.

### Acknowledgements

The PI of MAGDAS/CPMN project, K. Yumoto, SERC, Kyushu Univ. very much appreciates 30 organizations and Co-investigators around the world for their ceaseless cooperation and contribution to the MAGDAS/CPMN project. Financial supports were provided by Japan Society for the Promotion of Science (JSPS) as Grant-in-Aid for Overseas Scientific Survey (15253005, 18253005) and for publication of scientific research results (188068).

### References

- Baransky, L. N., Borovkov, J. E., Gokhberg, M. B., Krylov, M., & Troitskaya, V.A., 1985, P&SS, 33, 1369  
Baransky, L.N., Belokris, S.P., & Borovkov, J.E., 1990, P&SS, 38, 1573  
Ikeda, A., Shinohara, M., Yoshikawa, A., Nozaki, K., & Yumoto, K., 2006, Hokkaido Univ.  
Kohta, H., Uozumi, T., Kitamura, K., Yoshikawa, A., Shinohara, M., & Yumoto, K., MAGDAS Group, 2005, Proc. 118th SGEPS Fall Meeting, Kyoto Univ., B41-08

- Takasaki, S., Kawano, H., Tanaka, Y., Yoshikawa, A., Seto, M., Iijima, M., Obana, Y., Sato, N., & Yumoto, K., 2006, *E&PS*, 58, 617
- Tsurutani, B.T., Saito, A., Verkhoglyadova, O.P., Mannucci, A.J., Abdu, M.A., Araki, T., Gonzalez, W.D., Iijima, B.A., Lakhina, G.S., McCreadie, H., Soral, J.H.A., Tsuda, T., Yumoto, K., & Yasyliunas, V.M., 2006, *Solar Influence on the Heliosphere and Earth's Environment: Recent Progress and Prospects*, eds N. Gopalswamy & A. Bhattacharyya, ISBN-81-87099-40-2, pp. 384
- Uozumi, T., Yumoto, K., Kitamura, K., Abe, A., Kakinami, Y., Shinohara, M., Yoshikawa, A., Kawano, H., Ueno, T., & Tokunaga, T., MAGDAS Group, 2007, *E&PS*, 59 (in press)
- Waters, C.L., Menk, F.W., & Fraser, B.J., 1991, *GeoRL*, 18, 17547
- Yumoto, K., 1985, *P&SS*, 24, 1029
- Yumoto, K., 1988, *JGG*, 40, 293
- Yumoto, K., 2004, *Advances in Solar-Terrestrial Physics*, edited by H. Oya, TERRAPUB, Tokyo, pp.175-211
- Yumoto, K., 210° MM group, 1995, *JGG*, 47, 1197
- Yumoto K., 210° MM group, 1996, *JGG*, 48, 1297
- Yumoto, K., CPMN group, 2001, *E&PS*, 53, 981
- Yumoto, K., MAGDAS group, 2006, *Solar Influence on the Heliosphere and Earth's Environment: Recent Progress and Prospects*, eds N. Gopalswamy & A. Bhattacharyya, ISBN-81-87099-40-2, pp. 399